Sec61 blockade by mycolactone inhibits antigen cross-presentation independently of endosome-to-cytosol export

Jeff E. Grotzke[a,1], Patrycja Kozik[b,1,2], Jean-David Morel[c,d,1], Francis Impens[e,f,g], Natalia Pietrosemoli[h], Peter Cresswell[a,i,3,4], Sebastian Amigorena[b,j,k,3,4], and Caroline Demangel[c,d,3,4]

[a]Department of Immunobiology, Yale University School of Medicine, New Haven, CT 06520; [b]Centre de Recherche, Institut Curie, 75005 Paris, France; [c]Immunobiology of Infection Unit, Institut Pasteur, 75015 Paris, France; [d]INSERM, U1221, 75005 Paris, France; [e]Vlaams Instituut voor Biotechnologie (VIB)-UGent Center for Medical Biotechnology, 9000 Ghent, Belgium; [f]VIB Proteomics Core, 9000 Ghent, Belgium; [g]Department of Biochemistry, Ghent University, 9000 Ghent, Belgium; [h]Center of Bioinformatics, Biostatistics, and Integrative Biology, Institut Pasteur, Unité de Service et de Recherche 3756 Institut Pasteur CNRS, 75015 Paris, France; [i]Department of Cell Biology, Yale University School of Medicine, New Haven, CT 06520; [j]INSERM, U932, 75005 Paris, France; and [k]CBT507 Institut Gustave Roussy-Curie, INSERM Center of Clinical Investigation, 75005 Paris, France

Contributed by Peter Cresswell, June 8, 2017 (sent for review March 29, 2017; reviewed by Jose A. Villadangos and Emmanuel J. Wiertz)

Although antigen cross-presentation in dendritic cells (DCs) is critical to the initiation of most cytotoxic immune responses, the intracellular mechanisms and traffic pathways involved are still unclear. One of the most critical steps in this process, the export of internalized antigen to the cytosol, has been suggested to be mediated by Sec61. Sec61 is the channel that translocates signal peptide-bearing nascent polypeptides into the endoplasmic reticulum (ER), and it was also proposed to mediate protein retrotranslocation during ER-associated degradation (a process called ERAD). Here, we used a newly identified Sec61 blocker, mycolactone, to analyze Sec61's contribution to antigen cross-presentation, ERAD, and transport of internalized antigens into the cytosol. As shown previously in other cell types, mycolactone prevented protein import into the ER of DCs. Mycolactone-mediated Sec61 blockade also potently suppressed both antigen cross-presentation and direct presentation of synthetic peptides to $CD8^+$ T cells. In contrast, it did not affect protein export from the ER lumen or from endosomes into the cytosol, suggesting that the inhibition of cross-presentation was not related to either of these trafficking pathways. Proteomic profiling of mycolactone-exposed DCs showed that expression of mediators of antigen presentation, including MHC class I and β2 microglobulin, were highly susceptible to mycolactone treatment, indicating that Sec61 blockade affects antigen cross-presentation indirectly. Together, our data suggest that the defective translocation and subsequent degradation of Sec61 substrates is the cause of altered antigen cross-presentation in Sec61-blocked DCs.

Sec61 | cross-presentation | ERAD | mycolactone

Dendritic cells (DCs) play a key role in initiation of cytotoxic immune responses against pathogens and tumors (1). To prime relevant T cells, DCs capture antigens released by the surrounding cells and present them in the context of MHC class I (MHC-I) molecules (2). This process is referred to as cross-presentation and, in presence of appropriate costimulatory signals, leads to the activation and proliferation of antigen-specific T cells. Over recent years, extensive research efforts have gone into understanding the molecular mechanism of cross-presentation. The picture that emerged is that efficient cross-presentation requires antigens to be protected from excessive lysosomal degradation and, instead, to be exported into the cytosol for processing by the proteasome (3). Proteasomes generate short peptides that can then be presented on MHC-I. The molecular machinery that controls the step of antigen export from endosomes into the cytosol remains elusive, and the underlying mechanism is controversial. Interestingly, several groups have described that components of endoplasmic reticulum (ER)-associated degradation (ERAD) machinery are recruited to antigen-containing compartments (reviewed in ref. 4). These observations have led to the hypothesis that antigen export might "hijack" a channel used during retrotranslocation of misfolded proteins from the ER during ERAD.

The ERAD process uses a multiprotein complex consisting of lectins, chaperones, disulfide isomerases, E3 ubiquitin ligases, and other accessory factors (5). Once a terminally misfolded protein is recognized by the ERAD machinery, it is targeted to the ERAD membrane complex and ubiquitinated by an E3 ligase, such as Hrd1, during translocation into the cytosol, with the aid of the cytosolic AAA-ATPase p97, and subsequently degraded by the proteasome. Although the function(s) of many ERAD factors are at least partially understood, the precise identity of the pore that mediates cytosolic translocation remains unclear. In addition to its role in co- or posttranslational translocation of secretory proteins, Sec61 has long been proposed to be a potential translocon for dislocation of ERAD substrates from the ER. Experimental evidence supporting this model

Significance

Aside from its undisputed role in the import of newly synthesized proteins into the endoplasmic reticulum (ER), the Sec61 translocon was proposed to ensure the reverse transport of misfolded proteins to the cytosol. Based on this model, Sec61 was also proposed to be the channel exporting internalized antigens from endosomes to the cytosol, for degradation and cross-presentation. Establishing Sec61's contribution to these connected trafficking pathways has nevertheless proven difficult, due to a technical incapacity to blunt its activity acutely. Here, we took advantage of a recently identified Sec61 blocker to determine whether or not Sec61 can mediate retrograde protein transport. Both ER-to-cytosol and endosome-to-cytosol protein export were intact in mycolactone-treated cells, which argues against Sec61 operating as a retrotranslocon.

Author contributions: J.E.G., P.K., J.-D.M., P.C., S.A., and C.D. designed research; J.E.G., P.K., J.-D.M., F.I., and N.P. performed research; P.C. and C.D. contributed new reagents/analytic tools; S.A. analyzed data; J.E.G., P.K., S.A., and C.D. wrote the paper; and P.C. supervised the work performed at Yale University.

Reviewers: J.A.V., The University of Melbourne; and E.J.W., University Medical Center Utrecht.

The authors declare no conflict of interest.

[1]J.E.G., P.K., and J.-D.M. contributed equally to this work.

[2]Present address: Medical Research Council Laboratory of Molecular Biology, CB2 0QH Cambridge, United Kingdom.

[3]P.C., S.A., and C.D. contributed equally to this work.

[4]To whom correspondence may be addressed. Email: peter.cresswell@yale.edu, sebastian.amigorena@curie.fr, or demangel@pasteur.fr.

This article contains supporting information online at www.pnas.org/lookup/suppl/doi:10.1073/pnas.1705242114/-/DCSupplemental.

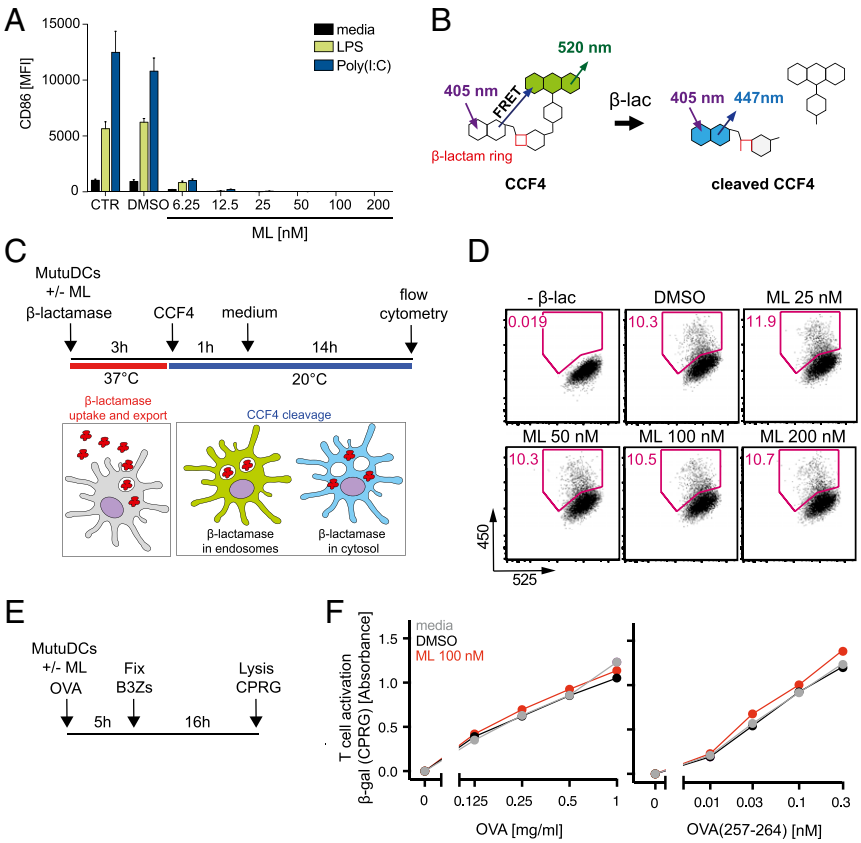

Fig. 1. Acute inhibition of Sec61 with mycolactone (ML) does not inhibit antigen export or cross-presentation. (*A*) ML efficiently prevents the TLR4- or TLR3-induced production of Sec61 substrates in MutuDCs. Cells were activated by 0.5 μg/mL LPS or 5 μg/mL high-molecular-weight poly(I:C) and incubated in the presence of 100 nM ML for 16 h. CTR, control; MFI, mean fluorescence intensity. Up-regulation of CD86 surface expression was monitored by flow cytometry. (*B*) Schematic representation of changes in CCF4 fluorescence upon cleavage of the the β-lactam (β-lac) ring. (*C*) Schematic representation of the antigen export assay. MutuDCs are fed with the β-lactamase and loaded with CCF4 in *B*, and the efficiency of CCF4 cleavage is analyzed by flow cytometry. (*D*) MutuDCs were incubated with β-lac in the presence or absence of increasing concentrations of ML for 3 h and analyzed as described in *C*. (*E*) Schematic representation of the cross-presentation assay. (*F*) MutuDCs were incubated for 5 h with soluble OVA protein or $OVA_{257–264}$ peptide in the presence or absence of increasing concentrations of ML. DCs were then fixed and coincubated with B3Z hybridomas for 16 h. Up-regulation of β-galactosidase (β-gal) expression in B3Zs (driven by the IL-2 promoter) was quantified using a colorimetric substrate, CPRG. For *D* and *F*, representative data from three independent experiments are shown.

was predominantly from yeast Sec61 mutants that are defective in both import of secretory proteins and export of ERAD substrates (6). Furthermore, a Sec61 mutant without defects in protein import but with reduced ability to bind to the 19S proteasome regulatory particle (RP) showed decreased ER export of a 19S proteasome RP-dependent substrate when proteasomes were limiting, providing a functional link between Sec61 and retrotranslocation (7). However, overexpression of the yeast E3 ubiquitin ligase Hrd1p can reduce or abolish the requirement of accessory ERAD factors, and Hrd1p is sufficient for substrate translocation in reconstituted proteoliposomes (8), arguing that Hrd1p is the protein channel for ERAD substrates. Whether these findings using yeast Sec61p and Hrd1p extrapolate to their mammalian counterparts remains to be demonstrated. Based on this model, several groups proposed that Sec61 might also play a role in antigen export from endosomes to the cytosol in DCs (9, 10). In support of this hypothesis, siRNA-mediated depletion of Sec61, or Sec61 exclusion from antigen-containing endosomes with an intrabody, inhibited antigen export into the cytosol, as well as cross-presentation (11, 12). However, these studies did not take into account the contribution of Sec61 to translocation of newly synthesized proteins into the ER, as well as the potential "knock-on" effects.

To investigate direct vs. indirect effects of Sec61 blockade, we used a pharmacological approach. Mycolactone is a polyketide-derived macrolide produced by the human pathogen *Mycobacterium ulcerans*, which was recently identified as a potent Sec61 inhibitor (13–16). Mycolactone diffuses passively across the plasma membrane to target the pore-forming subunit of the translocon (Sec61α) (13), leading to the proteasomal degradation of newly synthesized Sec61 clients blocked in translocation (17). In contrast to previously described Sec61 inhibitors, such as cotransin (18), mycolactone prevents the biogenesis of secretory and transmembrane proteins with minor selectivity toward Sec61 substrates, as well as uniformly high efficacy (13, 16). Single-amino acid mutagenesis localized its binding site on the luminal side of the translocon, near the plug domain that occludes Sec61 in its inactive state (13). Mycolactone allows acute blockade of Sec61, and we used it in the present study to examine the direct contribution of this channel to antigen cross-presentation, endosome-to-cytosol export, and ER-to-cytosol export.

Results

Acute Inhibition of Sec61 Does Not Block Antigen Export and Cross-Presentation. As a DC model, we used a $CD8^+$ cell line called MutuDC that was shown to display the phenotypic and functional features of splenic $CD8^+$ conventional DCs, including cross-presentation (19). We reported previously that mycolactone blocks the activation-induced maturation of peripheral

blood- and bone marrow-derived DCs, as evidenced by the up-regulation of costimulatory molecules (20). In MutuDCs activated with the TLR4 agonist LPS, or with the TLR3 agonist polyinosinic-polycytidylic acid [poly(I:C)], up-regulation of the cell surface expression of CD86 after 24 h was abrogated by coincubation with 6 nM mycolactone, showing that Sec61 blockade is effective in this DC model (Fig. 1*A*). Of note, no cytotoxicity could be detected in MutuDCs treated with up to 400 nM mycolactone for 24 h (Fig. S1*A*). To evaluate the effect of Sec61 blockade on antigen export from endosomes into the cytosol, we used a previously described β-lactamase–based assay that relies on a cytosolic dye (CCF4) consisting of two fluorophores linked by a β-lactam ring (21) (Fig. 1*B*). Upon excitation with a 405-nm laser, CCF4 emits green fluorescence due to the FRET between the two subunits. When β-lactamase is exported into the cytosol, it cleaves the β-lactam ring in CCF4, resulting in loss of FRET and change in fluorescence emission from green to blue (Fig. 1*B*). Here, we fed MutuDCs with β-lactamase in the presence or absence of increasing concentrations of mycolactone for 3 h, and subsequently loaded the cells with CCF4 (Fig. 1*C*). To increase the sensitivity of the assay, following CCF4 loading, we incubated the cells overnight at room temperature. The green-to-blue fluorescence transition was monitored by flow cytometry. No detectable difference in fluorescence could be demonstrated between mycolactone-treated and vehicle control cells, indicating that Sec61 blockade by mycolactone does not affect antigen export (Fig. 1*D* and Fig. S1*B*).

The DCs were then fixed and incubated for 16 h with the T-cell hybridoma B3Z, which expresses T-cell receptor specific for a complex of the MHC-I Kb allele with ovalbumin 257–264 ($OVA_{257–264}$) peptide (Fig. 1*E*). B3Z activation leads to accumulation of β-galactosidase reporter, which is expressed under transcriptional control of the NFAT elements from the IL-2 promoter. β-Galactosidase levels were quantified using a colorimetric substrate, chlorophenol red-β-D-galactopyranoside (CPRG). To ensure that B3Z activation itself was not affected by mycolactone, we used a B3Z line expressing the R66G mycolactone-resistant mutant of Sec61 (Sec61-R66G), generated as described (13). We observed no difference in the efficiency of OVA cross-presentation or in the capacity of DCs to activate T cells when incubated directly with the $OVA_{257–264}$ peptide (Fig. 1*F*). Together, these data thus suggest that acute inhibition of Sec61 does not block antigen export or cross-presentation.

Deglycosylation-Dependent ERAD Substrates Are Differentially Affected by Mycolactone. We next investigated whether mycolactone-mediated Sec61 inhibition affected the export of proteins from the ER into the cytosol during ERAD. To achieve this goal, we used

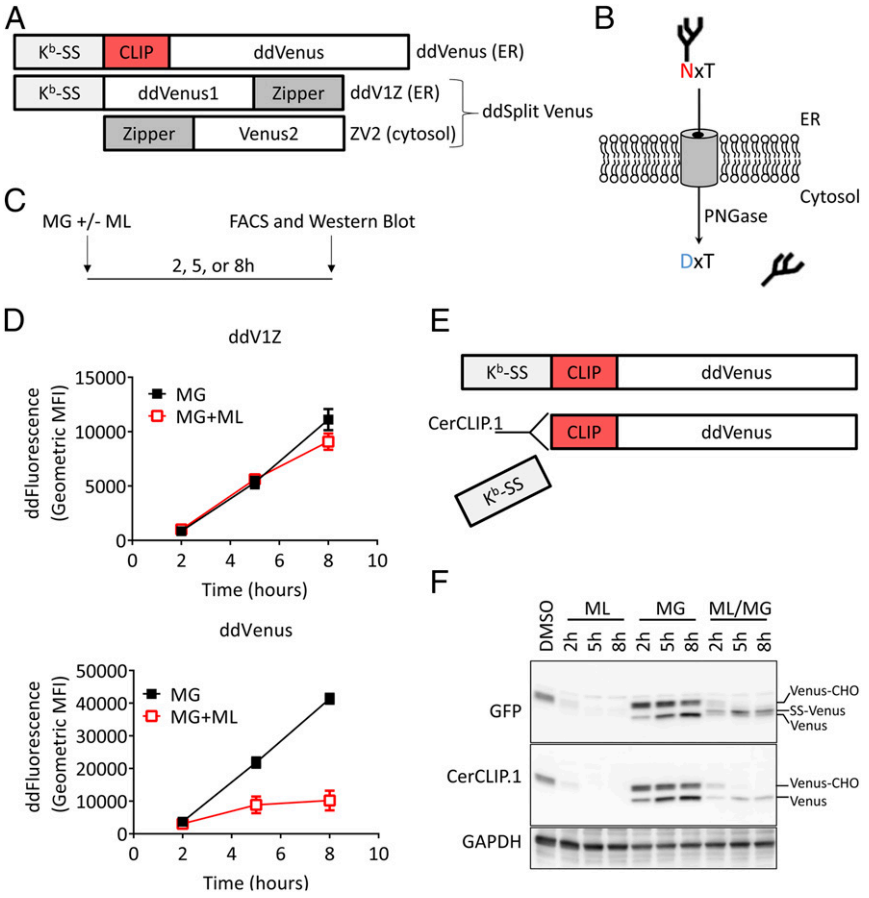

Fig. 2. ERAD dd substrates are differentially affected by ML. (*A*) Constructs used in Fig. 2. The dd substrates are targeted to the ER through fusion to the signal sequence of H2-Kb (Kb-SS). Dimerization of split Venus halves is driven through fusion of both halves to leucine zippers. (*B*) Depiction of dd substrate mechanism. Removal of the N-linked glycan by cytosolic PNGase leads to asparagine deamidation and conversion to an aspartic acid, restoring Venus fluorescence. (*C*) Experimental design. MG, MG-132. (*D*) HEK293T cells stably expressing dd substrates were treated with 4 μM MG ± 100 nM ML for the times indicated. At each time point, cells were harvested and fluorescence was analyzed by flow cytometry. The level of dd fluorescence was quantitated by flow cytometry, as described in *Materials and Methods*. (*E*) Recognition of the CLIP epitope by the monoclonal antibody CerCLIP.1 requires a free N terminus. (*F*) HEK293T cells expressing ddVenus were treated as in *D*, and cell lysates were analyzed by Western blot using antibodies to GFP, which reacts with Venus, and the CLIP epitope. Different forms of Venus are indicated.

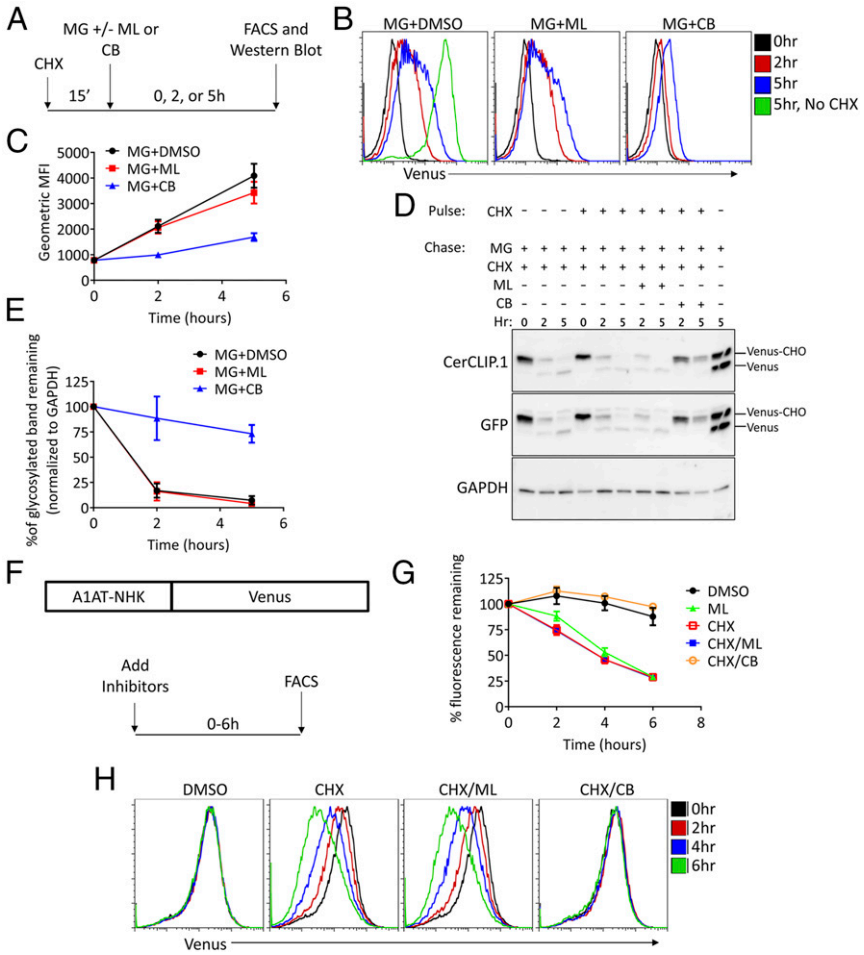

Fig. 3. ML-mediated Sec61 blockade does not inhibit retrotranslocation of ERAD substrates. (*A*) Experimental design for *B*–*E*. (*B*–*E*) HEK293T cells stably expressing ddVenus were pulsed for 15 min with 20 μg/mL cycloheximide (CHX), followed by addition of 4 μM MG ± 100 nM ML or 1 μM CB-5083 (CB). At each time point, cells were harvested and analyzed by flow cytometry (*B* and *C*) or cell lysates were analyzed by Western blot (*D* and *E*). Time 0 (pulse CHX, chase MG+CHX, fourth lane from the left in *D*) was the same for all CHX-pulsed treatments in *D* and *E*. Results in *C* and *E* are the mean ± SEM of at least three independent experiments. (*F*) Construct and experimental design used in *G* and *H*. Wild-type Venus was fused to the N terminus of A1AT-NHK. (*G* and *H*) HEK293T cells stably expressing A1AT-NHK-Venus were treated with 20 μg/mL CHX ± 100 nM ML or 1 μM CB for the indicated times. At each time point, cells were harvested and analyzed by flow cytometry. Results in *H* are the mean ± SEM of at least three independent experiments.

the previously described deglycosylation-dependent (dd) ERAD substrate constructs ddVenus and ddSplit Venus (22) as fluorescent reporters of ERAD activity (Fig. 2*A*). In ddSplit Venus, half of Venus (ddV1Z) is targeted to the ER, whereas the other half (ZV2) is expressed in the cytosol. Both ddVenus and ddSplit Venus were engineered with an N-linked glycosylation site in which an aspartic acid in the wild-type sequence was mutated to an asparagine, resulting in reduced fluorescence. After glycosylation in the ER, substrates that are retrotranslocated to the cytosol are deglycosylated by peptide N′-glycanase (PNGase), resulting in deamidation of the asparagine (red in Fig. 2*B*) and conversion back to the wild-type aspartic acid (blue in Fig. 2*B*), yielding enhanced fluorescence. Cells expressing dd substrates are nonfluorescent at steady state because the substrates are degraded by proteasomes, but cellular fluorescence (ERAD) can be detected after the addition of proteasome inhibitors. This cellular fluorescence requires the ERAD factors Hrd1 and SEL1L, as well as PNGase activity. To determine the effect of mycolactone-mediated Sec61 blockade on ERAD, we used cells stably expressing ddVenus or ddSplit Venus (Fig. 2*A*). Cells were incubated with the proteasome inhibitor MG-132 in the presence or absence of mycolactone for 2–8 h (Fig. 2*C*). When the fluorescence of ddV1Z and ddVenus was quantitated in treated cells, mycolactone, surprisingly, showed different effects on the two substrates. Although fluorescence was largely inhibited for ddVenus, only a slight nonstatistically significant effect was seen at 8 h posttreatment for ddSplit Venus (Fig. 2*D*). With both substrates, fluorescence was decreased by coincubation of the cells with the PNGase inhibitor zVAD-fmk (Fig. S2*A*), showing that it is deglycosylation-dependent. These results suggested that Sec61 blockade differentially affects ERAD of the two substrates.

We tested if mycolactone had different effects on the stability and glycosylation state of ddVenus and ddV1Z by Western blot analysis of cell lysates, as glycosylated (-CHO) and non-glycosylated or deglycosylated species have different molecular weights. Using an anti-GFP antibody cross-reacting with Venus, we found that mycolactone treatment caused a time-dependent depletion of the glycosylated form of ddV1Z (V1Z-CHO; Fig. S2*B*), indicating that ddV1Z translocation into the ER was blocked. Consistent with this finding, mycolactone treatment also caused the appearance of a species that migrated slightly slower than the nonglycosylated or deglycosylated species [labeled signal sequence (SS)-V1Z, compared with V1Z]. This species is likely cytosolically translated ddV1Z with an uncleaved signal sequence (discussed below), and it is stabilized even further in the presence of MG-132. To confirm further that mycolactone was able to block ddV1Z translocation into the ER, we

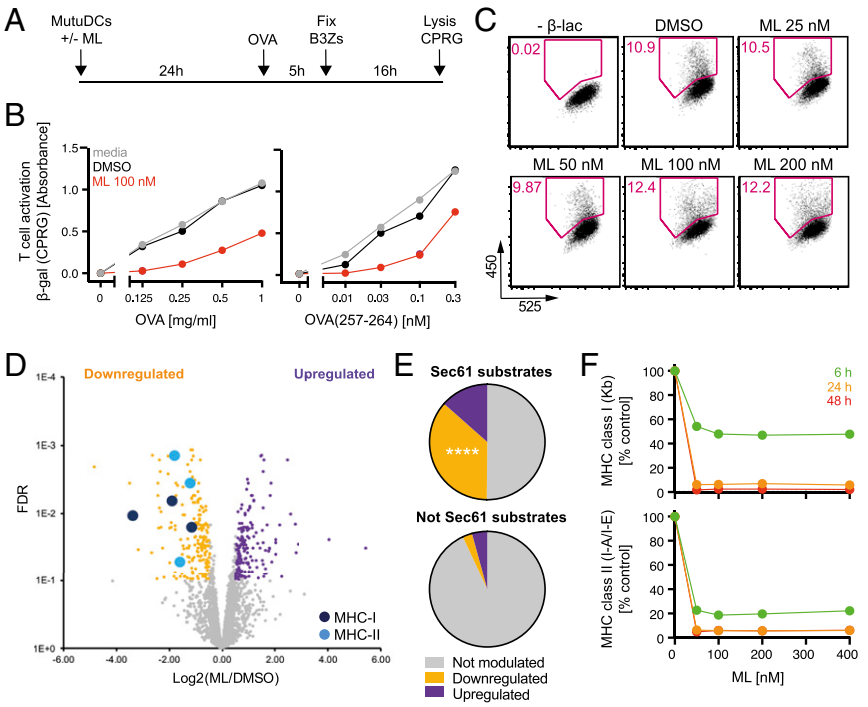

Fig. 4. Prolonged inhibition of Sec61 with ML diminishes T-cell activation capacity of MutuDCs. (*A*) Schematic representation of the assay used in *B*. (*B*) MutuDCs were treated for 24 h with 100 nM ML, reseeded, and incubated with OVA or $OVA_{257–264}$ peptide for 5 h. The efficiency of T-cell activation was quantified as in Fig. 1*F*. (*C*) MutuDCs were treated with ML for 24 h, and the export assay was performed as described in Fig. 1 *B* and *C*. (*D*) Volcano plot showing statistical significance vs. fold change differences for each protein identified in MutuDCs treated with 100 nM ML or vehicle control for 24 h. (*E*) Pie charts depicting the proportion of down-regulated, up-regulated, or not modulated proteins among Sec61 substrates and all other identified proteins (not Sec61 substrates). ****$P < 0.0001$, Fisher exact test comparing the proportion of down-regulation in Sec61 substrates and all other identified proteins. (*F*) FACS analysis of MHC-I and MHC-II surface expression by MutuDCs treated with increasing doses of ML for 6, 24, and 48 h. For *B*, *C*, and *F*, representative data are from three independent experiments.

treated cells with mycolactone or DMSO for 8 h, and glycosylated proteins were depleted from cell lysates using Sepharose beads conjugated to Con A. Although there appeared to be some level of nonspecific binding to Con A beads, Fig. S2*C* clearly shows that mycolactone decreased the glycosylated form of ddV1Z (V1Z-CHO, lanes 1 and 4) and that the mycolactone-induced species was nonglycosylated (SS-V1Z, lane 5). Similarly, mycolactone potently depleted glycosylated HLA-I from treated cells (Fig. S2*C*). Both of these findings are consistent with a lack of ER import. Overall, these data demonstrate that mycolactone blocks the import of ddV1Z into the ER with little to no effect on export and suggest that Sec61 does not play a role in ERAD of this substrate.

In contrast to ddV1Z, ddVenus was rapidly depleted by mycolactone treatment, with little to no protein detectable after 5 h (GFP panel in Fig. 2*F*). To discriminate between signal sequence-cleaved and -uncleaved species, we assessed cell lysates for the presence of ddV1Z proteins containing the CLIP (class II-associated invariant chain peptide) epitope, which is inserted between the signal sequence and ddVenus (Fig. 2*A*). We used the antibody CerCLIP.1, which requires a free amino terminus to bind CLIP, and therefore only detects signal sequence-cleaved ddVenus (Fig. 2*E*). In ddVenus cells cotreated with mycolactone and MG-132, there was an appearance of the same slower migrating species as seen in ddV1Z (SS-Venus; Fig. 2*F*). This band was detected with an antibody to GFP, but not with CerCLIP.1, demonstrating that it represents protein translated in the cytosol with an intact signal sequence. These data suggest that differences in substrate half-life may explain the contrasting effect of mycolactone on ddV1Z vs. ddVenus, but the possibility remained that Sec61 was required for ddVenus export.

Mycolactone-Mediated Sec61 Blockade Does Not Inhibit Retrotranslocation of ERAD Substrates. To distinguish between the role of Sec61 in import and export, we assessed the ability of the preformed ER pool of ddVenus to be retrotranslocated to the cytosol. Cells were pulsed with cycloheximide for 15 min to prevent protein synthesis, and then chased with MG-132 ± mycolactone or CB-5083, a potent p97 inhibitor (23), in the continued presence of cycloheximide (Fig. 3*A*). As shown in Fig. 3 *B* and *D*, cycloheximide markedly reduced both the level of cellular fluorescence and the levels of glycosylated and deglycosylated ddVenus, arguing that the majority of ddVenus fluorescence arises from nascent protein. No significant differences in fluorescence were seen between the cells cotreated with MG-132 and DMSO or mycolactone (Fig. 3 *B* and *C*). Similarly, mycolactone did not stabilize the glycosylated ddVenus band or inhibit the transition of the glycosylated band to the deglycosylated form (Fig. 3 *D* and *E*). CB-5083–mediated inhibition of p97, a protein required for extraction of ERAD substrates from the ER, led to decreased cellular fluorescence, stabilization of glycosylated ddVenus, and lack of deglycosylated ddVenus (Fig. 3 *D* and *E*). Taken together, these results demonstrate that ddVenus fluorescence inhibition by mycolactone is due to decreased levels of nascent substrate and not due to blockade of the ERAD translocon.

Finally, we assessed the ability of mycolactone to block ERAD of an additional substrate, the Null Hong Kong variant of α1-antitrypsin (24) fused to Venus (A1AT-NHK-Venus) (Fig. 3*F*). Unlike the dd substrates, this substrate is fluorescent whether present in the ER or cytosol. We reasoned that if mycolactone blockade of Sec61 prevents export to the cytosol, then it should stabilize the ER pool of A1AT-NHK-Venus when protein synthesis is inhibited. As shown in Fig. 3 *G* and *H*, cycloheximide

Table 1. Effect of mycolactone treatment on known mediators of cross-presentation

FDR	Variation*	Protein name†	Gene name†	Sec61 substrate
3.20E-03	1.89	Protein transport protein Sec61 subunit α1	Sec61a1	Yes
2.58E-02	1.78	Vesicle-associated membrane protein 8	Vamp8	No
1.45E-02	1.65	Heat shock protein (HSP) 90-α	Hsp90aa1	No
6.41E-02	1.52	Ras-related protein Rab-35	Rab35	No
5.43E-02	1.37	HSP 90-β	Hsp90ab1	No
2.21E-01	1.27	Ras-related protein Rab-8B	Rab8b	No
1.61E-01	1.23	AP-3 complex subunit δ1	Ap3d1	No
2.84E-01	1.22	Ras-related protein Rab-10	Rab10	No
4.30E-01	1.20	Proteasome subunit β type 9	Psmb9	No
4.84E-01	1.17	TNF receptor-associated factor 6	Traf6	No
3.85E-01	1.16	Ras-related protein Rab-6A or Rab6b	Rab6a, Rab6b	No
7.59E-01	1.08	Wiskott–Aldrich syndrome protein homolog	Was	No
8.15E-01	1.07	Antigen peptide transporter 1	Tap1	Yes
8.05E-01	1.05	AP-3 complex subunit β1	Ap3b1	No
4.41E-01	1.38	Protein transport protein Sec61 subunit γ	Sec61g	No
8.90E-01	1.03	Synaptosomal-associated protein 23	Snap23	No
9.33E-01	1.01	Large proline-rich protein BAG6	Bag6	No
6.42E-01	1.49	Ras-related protein Rab-5B	Rab5b	No
5.28E-01	0.67	Derlin-1	Derl1	Yes
8.89E-01	0.98	Ras-related protein Rab-11B	Rab11b	No
9.29E-01	0.98	Proteasome subunit β type 8	Psmb8	No
7.04E-01	0.95	Proteasome activator complex subunit 1	Psme1	No
7.69E-01	0.93	Antigen peptide transporter 2	Tap2	Yes
9.35E-01	0.93	H2 MHC-II, E-Q, I-A, E-B, or E-S β chain	H2-Eb1	Yes
1.93E-01	0.86	Transitional ER ATPase	Vcp/p97	No
3.87E-01	0.75	IgG receptor FcRn large subunit p51	Fcgrt	Yes
9.81E-01	0.97	MHC-II, M β1 chain	H2-DMb1	Yes
3.66E-01	0.79	Tapasin	Tapbp	Yes
7.54E-02	0.74	ER aminopeptidase 1	Erap1	Yes
3.27E-02	0.58	γ-IFN–inducible lysosomal thiol reductase	Ifi30	Yes
2.24E-02	0.55	Intercellular adhesion molecule 1	Icam1	Yes
2.88E-02	0.54	Cathepsin S	Ctss	Yes
1.62E-02	0.44	H2 MHC-I, D-B α chain	H2-D1	Yes
3.65E-03	0.42	H2 MHC-II, A or A-U β chain	H2-Ab1	Yes
5.24E-02	0.32	H2 MHC-II γ chain	Cd74	Yes
1.41E-03	0.28	H2 MHC-II, A-B or A-U α chain	H2-Aa	Yes
6.62E-03	0.26	H2 MHC-I, K-B or K-K α chain	H2-K1	Yes
1.07E-02	0.09	β2 microglobulin	B2m	Yes

Proteins that were significantly up-regulated [FDR ≤ 0.1; $\log_2$(variation) > 0.5] or down-regulated [FDR ≤ 0,1; $\log_2$(variation) < −0.5] by mycolactone are highlighted in dark gray and light gray, respectively. FcRn, neonatal Fc receptor.

*Fold change (mycolactone/control).

†According to www.uniprot.org.

caused a gradual loss of A1AT-NHK-Venus over the 6-h course of the experiment. This reduction in fluorescence was mediated by ERAD, because it was inhibited by CB-5083. When cells were cotreated with cycloheximide and mycolactone, no difference was seen in A1AT-NHK-Venus stability compared with when cells were treated with cycloheximide alone. In all, our data using three different ERAD substrates demonstrate that although blockade of Sec61 can mediate apparent decreases in ERAD, these effects are due to depletion of the pool of ERAD substrates without an obvious effect on substrate retrotranslocation.

Sec61 Blockade Affects the Production of Key Mediators of Antigen Cross-Presentation. The observed lack of an effect of Sec61 inhibition on antigen cross-presentation was inconsistent with previous data obtained with Sec61-depleted cells (11, 12). Because acute blockade of Sec61 failed to inhibit substrate export both from the endosomes and from the ER, we hypothesized that prolonged Sec61 inhibition could lead to defects in cross-presentation, similar to siRNA-depleted cells. Indeed, when MutuDCs were pretreated with mycolactone for 24 h (Fig. 4*A*), we observed a strong decrease in cross-presentation efficiency (Fig. 4*B*). However, there was a similar decrease in the efficiency of B3Z activation when mycolactone-treated DCs were incubated directly with the $OVA_{257–264}$ peptide (Fig. 4*B*). Furthermore, this decrease in capacity of DCs to activate T cells did not correlate with inhibition of antigen export into the cytosol (Fig. 4*C*). Together, these data imply that prolonged inhibition of Sec61 decreases the overall capacity of DCs to present antigens in the context of MHC-I molecules, rather than antigen export and cross-presentation specifically.

We hypothesized that the inhibition of Sec61-mediated ER import, rather than retrotranslocation, might contribute to the decrease in the capacity of DCs to present antigens. Therefore, we next monitored the proteome of Sec61-blocked MutuDCs over time, using a label-free quantitative approach. Triplicate cell extracts were prepared from MutuDCs exposed to 100 nM mycolactone or vehicle control for 6 or 24 h. Proteins were trypsin-digested, and peptide mixtures processed were analyzed by LC-tandem MS (MS/MS). The proteomic analysis of cell lysates identified 4,197 proteins, among which 3,206 could be

reproducibly quantified across replicates. With the single exception of Akt2, none of these proteins was significantly modulated after 6 h of mycolactone treatment (data not shown for clarity). However, after 24 h, 204 proteins were down-regulated in mycolactone-treated MutuDCs, whereas 170 proteins were up-regulated (Fig. 4*D* and Table S1). Consistent with Sec61 inhibition, a large proportion of Sec61 substrates (36%) were down-regulated in response to mycolactone, compared with 2% of all other proteins (Fig. 4*E*). We examined in greater detail whether known mediators of antigen cross-presentation were affected, either negatively or positively, by Sec61 blockade. Fig. 4*D* and Table 1 show that the subunits of the MHC-I and MHC-II molecules [heavy chain (H2-Kb and H2-Db) and β_2 microglobulin for MHC-I, α (H2-IAα) and β (H2-Aβ1) chains for MHC-II] were among the most efficiently down-regulated proteins. A flow cytometric analysis of mycolactone-treated MutuDCs confirmed these findings (Fig. 4*F*). Importantly, 24 h of exposure to >50 nM mycolactone caused >90% loss of both MHC-I (H2-Kb) surface expression (orange line in Fig. 4*F*), providing an explanation for the defective capacity of mycolactone-treated MutuDCs to cross-present antigens to $CD8^+$ T cells, as seen in Fig. 4*B*. In contrast, MHC-I expression was only partially affected after 6 h of mycolactone treatment (green line in Fig. 4*F*), which is consistent with the unaltered capacity of MutuDCs to cross-present antigen in the conditions of acute Sec61 inhibition used in Fig. 1*F*. Together, the data in Figs. 1 and 4 are thus fully consistent with Sec61 blockade affecting antigen cross-presentation indirectly.

Discussion

The molecular mechanism responsible for antigen exit from endosomes and phagosomes during cross-presentation has been a matter of debate for over 20 y. Sec61 emerged as a promising candidate for an exit channel after it was detected in phagosomes (25–27) and functionally associated with retrotranslocation of proteins from the ER to the cytosol (28). Indeed, suppression of Sec61 in knockdown experiments reduced antigen export to the cytosol to some extent, and inhibited antigen cross-presentation strongly (11, 12). Reduced Sec61 activity, however, is also expected to prevent translocation of secreted proteins into the ER, and thereby to affect numerous cell functions indirectly. To minimize the indirect effects of Sec61 blockade, we have used a pharmacological approach based on mycolactone, a specific Sec61α binder and potent Sec61 blocker. Acute Sec61 blockade by mycolactone severely inhibited the import of secreted proteins into the ER in DCs, but did not interfere with ERAD or protein export from endocytic compartments. Sustained, but not short-term, Sec61 blockade with mycolactone decreased the efficiency of antigen cross-presentation. Mycolactone also strongly inhibited T-cell activation by synthetic peptides and MHC-I expression, implying a more general effect of the drug on the capacity of DCs to present antigens. These findings are consistent with the extensively characterized function of Sec61 in cotranslational protein translocation into the ER (29). They suggest that Sec61α, the translocon subunit targeted by mycolactone, is not directly involved in antigen export to the cytosol, ERAD, or antigen cross-presentation.

Because mycolactone did not inhibit ERAD, we cannot exclude the possibility that the drug blocks forward (from the cytosol to the lumen), but not retrograde (from the lumen to the cytosol), translocation by Sec61. Recent advances in the structural understanding of the opening and closing of the Sec61 channel do not provide a mechanism for how luminal substrates could drive Sec61 plug displacement, and render the channel permissive to peptides during ERAD or cross-presentation (30). The current view of mycolactone's mode of action is that its binding near the luminal plug of Sec61α maintains the complex in a closed conformation (13, 15), which would be expected to prevent protein transport bilaterally. The contribution of Sec61 to substrate dislocation during ERAD in mammalian cells has been questioned repeatedly. Over the years, other mechanisms for retrotranslocation have been proposed, including novel putative channels (e.g., derlins, Hrd1) or lipid-based models (4). Although Sec61 components other than Sec61α may form part of the dislocation channel, our data support the view that the Sec61 complex is not the retrotranslocon for ERAD.

In contrast to this discrepancy between the effects of mycolactone (this study) and Sec61 knockdown (11, 12) on antigen export to the cytosol, both approaches caused inhibition of antigen cross-presentation. With regard to mycolactone, we show that direct presentation of a synthetic peptide (at low concentrations) is also inhibited upon blockade of Sec61. We also show that this result is due to reduced expression of MHC-I at the cell surface, a parameter that was not analyzed after knocking down Sec61 (12). Likewise, nanobodies used to retain Sec61 in the ER (12) could also inhibit protein translocation into the ER and MHC-I expression, altering antigen cross-presentation independent of antigen export to the cytosol. We note that decreased MHC-I expression is hard to detect using saturating concentrations of peptide.

Our proteomic analysis of mycolactone-exposed DCs also showed that many proteins involved in ERAD are significantly modulated after 24 h of Sec61 blockade (Table S2). Notably, accessory molecules that contribute to ERAD of the substrates used in this study [HERP, AUP1, and FAF2/UbxD8 (22, 25)] were up-regulated. These proteins likely belong to the small subset of Sec61 clients resisting mycolactone inhibitory activity, and their accumulation in treated DCs may reflect a stress response to ER translocation defects (13, 16). Increased levels of these factors are unlikely to confound our results, because we analyzed ERAD within 6 h of mycolactone treatment, a time at which these factors were not modulated in mycolactone-treated T cells or DCs (ref. 13 and this study). In contrast, the Sec61 substrates Endoplasmin, Erdj3, and OS-9 were significantly down-regulated in mycolactone-treated DCs, showing that Sec61 blockade not only limits the availability of ERAD substrates but also the availability of ERAD mediators. In all, the changes shown in Tables S1 and S2 demonstrate the large-scale alterations in the proteome that occur when Sec61 function is perturbed, and reinforce the argument that care must be taken when interpreting results showing functional defects in the face of Sec61 knockdown.

Interestingly, a substrate with a long half-life in the ER was unaffected by Sec61 blockade, whereas substrates with shorter half-lives were. When the export step of ER-localized ERAD substrates was examined, no effect of Sec61 blockade was observed. Hence, reduction of ERAD activity in mycolactone-treated cells was most likely due to reduced substrate import into the ER. Consistent with this finding, we detected the presence of nonglycosylated ERAD substrates with intact signal peptides in mycolactone-treated cells. Interestingly, we also detected the up-regulation of the cytosolic chaperones Hsp90α and HSP90β by proteomics. This result is likely due to the accumulation of ER-targeted proteins in the cytosol that are unable to fold properly in the absence of the ER-oxidizing environment, ER chaperones, and glycosylation machinery, and without membrane insertion to shield hydrophobic patches.

A critical role for Sec61 in protein export to the cytosol is also not fully consistent with the pore size that is required to support the export of functional fully folded proteins, such as β-lactamase or HRP, or heavily glycosylated proteins, such as OVA (31). If Sec61 is not involved, how then do antigens escape endocytic compartments in DCs? Recent studies suggest a role for reactive oxygen species and lipid peroxidation, which could locally destabilize the membrane of endocytic compartments, causing transient "leakage" into the cytosol (32). Local destabilization of the ER membrane through formation of lipid bodies was

suggested a few years ago to mediate ERAD (33). Lipid bodies were also shown to favor antigen cross-presentation (34), suggesting a possible link, independent of Sec61, between ERAD and antigen export of the cytosol. Although the search for the molecular mechanisms of ERAD and antigen export have been the object of sustained efforts for over 20 y, and even though Sec61 appeared to be a good candidate to support both, it is most likely that the search is not over.

Materials and Methods

Reagents and Constructs. Mycolactone A/B was purified from *M. ulcerans* bacteria (strain 1615; American Type Culture Collection 35840) and then quantified by spectrophotometry (λ_{max} = 362 nm, log ε = 4.29) (35). Stock solutions were prepared in DMSO and then diluted 1,000-fold in culture medium for cellular assays. The following inhibitors were used for analysis of the role of mycolactone in ERAD or antigen export: MG-132 (Enzo Life Sciences), cycloheximide (Sigma), CB-5083 (SelleckChem.com), zVAD-fmk (R&D Systems), and Eeyarestatin I (Sigma). Vectors encoding ERAD substrates have been described previously (22). The pRetroX-Sec61-IRES-Zsgreen vector used to transduce B3Z cells was derived from pRetroX-IRES-ZsGreen (Clontech) as described elsewhere (13). Flow cytometry reagents were anti-mouse MHC-I (H2-Kb)-phycoerythrin (PE) (12-5958-80; eBioscience), biotin-conjugated anti-mouse MHC-II (I-A/I-E) (553622; BD Biosciences), allophycocyanin-streptavidin (554067; BD Biosciences), anti-mouse CD86 PE-Cy7 (eBioscience 25-0862-82) and isotype control (eBioscience 25-4321-82). LPS (L4391; Sigma) was used at a final concentration of 0.5 μg/mL. High-molecular-weight poly(I:C) (AV-9030-10; Alpha Diagnostic) was preheated for 10 min at 70 °C and used at a final concentration of 5 μg/mL. DAPI was used at a final concentration of 0.5 μM. Fixable Viability Dye eFluor 780 (65-0865-14; eBioscience) was used at a ratio of 1:2,500 according to the manufacturer's instructions.

Cell Cultures. MutuDCs (kindly provided by Hans-Acha Orbea, University of Lausanne, Lausanne, Switzerland) were cultured in Iscove's modified Dulbecco's medium (12440-053; Gibco), supplemented with 8% (vol/vol) FCS (Biowest), 10 mM Hepes, 100 U/mL penicillin, 100 μg/mL streptomycin, and 50 μM β-mercaptoethanol (all from Life Technologies). B3Z hybridomas with a T-cell receptor specific to the Kb/$OVA_{257–264}$ peptide complex (kindly provided by Nilhab Shastri, University of California, Berkeley, CA) (36) were grown in RPMI, supplemented with 10% FCS, 2 mM GlutaMax, 10 mM Hepes, 1 mM sodium pyruvate, 1× nonessential amino acids, 100 IU/mL penicillin, 100 μg/mL streptomycin, and 50 μM β-mercaptoethanol. Mycolactone-resistant B3Z cells were generated as previously described (13). Briefly, Platinum E (Cell Biolabs) was transfected with the R66G-Sec61-IRES-Zsgreen vector using Fugene HD (Promega) as a transfection reagent. After 24 h, the retroviral supernatant was used to transduce B3Z cells, and R66G-Sec61–expressing cells were selected with mycolactone (200 nM). To generate stable cell lines expressing dd substrates, HEK293T cells were transiently transfected with the indicated ERAD substrates in pcDNA3.1-Zeo using Lipofectamine 2000 (both from Thermo Fisher Scientific) according to the manufacturer's suggestions. After 24–48 h, cells were selected with zeocin (Thermo Fisher Scientific) at 0.25–1 mg/mL to obtain stable integrants. Cells surviving selection were cloned by limiting dilution and screened for fluorescence after treatment with 4–8 μM MG-132 for 6 h. To obtain cells stably expressing A1AT-NHK-Venus, we first modified the retroviral vector pMXs-IRES-Puro (Cell Biolabs, Inc.) by replacing the puromycin resistance cassette with a zeocin resistance cassette, PCR-amplified from pcDNA3.1-Zeo, into the NcoI and SalI restriction sites. A1AT-NHK-Venus was PCR-amplified from pcDNA3.1-Zeo and cloned into the EcoRI site of pMXs-IRES-Zeo using the Gibson Assembly Cloning Kit (New England Biolabs). Retroviral supernatants were generated by cotransfection of pMXs-A1AT-NHK-Venus-IRES-Zeo and the packaging vector pCL-Ampho into HEK293T cells. After 48–72 h, supernatants containing retroviral particles were centrifuged at 500 × *g* for 10 min and filtered through a 0.45-μm filter. HEK293T cells were spinfected in the presence of polybrene (8 μg/mL; EMD Millipore) for 90 min at 32 °C. After 48 h, stable cells were selected with zeocin and cloned as above. Stable clones were maintained in DMEM (Thermo Fisher Scientific) supplemented with 10% FBS (Gemini Bioproducts), 2 mM GlutaMax, 50 U/mL penicillin, 50 μg/mL streptomycin, and 225 μg/mL zeocin (all from Thermo Fisher Scientific).

Analysis of Sec61 Blockade on Cross-Presentation. MutuDCs (100,000 per well) were incubated for 5 h with different concentrations of mycolactone and soluble grade VII OVA (no. A7641; Sigma Aldrich) or $OVA_{257–264}$ peptide. Next, MutuDCs were washed three times in PBS, fixed for 3 min with 0.008% glutaraldehyde solution in PBS (vol/vol), and washed twice with 0.2 M glycine. Finally, 100,000 B3Z hybridoma cells were added per well. After 16 h, the cells were lysed in a buffer containing 0.125% Nonidet P-40 (substitute) (sc-29102; Santa Cruz Biotechnology), 9 mM $MgCl_2$, and a colorimetric CPRG β-galactosidase substrate. The absorbance was measured at 590 nm.

Analysis of Sec61 Blockade on Antigen Export. MutuDCs were seeded at 200,000 cells per well in U-bottom, 96-well plates and incubated in the presence or absence of mycolactone with 10 mg/mL β-lactamase (no. P0389; Sigma) for 3 h at 37 °C. The cells were then washed and loaded with CCF4 for 45–60 min at room temperature (RT) as previously described (21). To increase the sensitivity of the assay, the DCs were then incubated for 16 h at RT in CO_2-independent media supplemented with 8% FCS and 2 mM GlutaMax. Immediately before flow cytometry analysis, the cells were stained with Fixable Viability Dye eFluor 780 (no. 65-0865-14; eBioscience) diluted at a ratio of 1:2,500 in PBS. The percentage of the live cells with a high blue-to-green (V450/V530) fluorescence ratio was used as a measure of the efficiency of antigen export into the cytosol.

Analysis of Sec61 Blockade on ERAD. HEK293T cells expressing ERAD substrates were plated at 50,000 cells per well in 96-well, flat-bottom plates and allowed to adhere overnight at 37 °C. Cells were treated alone or in combination with mycolactone (100 nM), MG-132 (4 μM), cycloheximide (20 μg/mL), CB-5083 (1 μM), and zVAD-fmk (20 μM) for the indicated times at 37 °C. For flow cytometry experiments, cells were harvested using trypsin/EDTA (Thermo Fisher Scientific), pooled into duplicate or triplicate wells, washed in PBS containing 2.5% FBS, and analyzed by means of Venus fluorescence on a BD Accuri C6 with autosampler (BD Biosciences). For Western blot analysis, cells from 96-well plates were washed in PBS and pellets were frozen at −20 °C. After thawing on ice, cells were lysed for 30 min in radioimmunoprecipitation assay buffer [50 mM Tris, 150 mM NaCl, 1% Nonidet P-40, 0.1% SDS, 0.5% sodium deoxycholate, and a Complete Protease Inhibitor tablet (Roche Life Sciences)]. Insoluble material was removed through centrifugation at 18,000 × *g* at 4 °C for 10 min. The soluble material was separated by SDS/PAGE on a 10–20% gradient gel (Thermo Fisher Scientific) and transferred to an Immobilon-P membrane (EMD Millipore). The membrane was blocked in 5% nonfat dry milk in Tris-buffered saline/0.05% Tween-20 (TBS-T) for 60 min, rinsed, and incubated with rabbit anti-GFP (A-6455; Thermo Fisher Scientific), CerCLIP.1 (37), or anti-GAPDH (6C5; Thermo Fisher Scientific) for 60 min of shaking at RT. Membranes were washed in TBS-T and incubated with alkaline phosphatase-conjugated secondary antibodies (Jackson Immunoresearch) for 60 min at RT. After three washes (10 min each wash) in TBS-T, membranes were incubated with ECF substrate (GE Healthcare Life Sciences) for 5 min at RT and imaged with a Typhoon FLA 9500 (GE Healthcare Life Sciences).

Role of Sec61 in Import or Export of ddVenus. HEK293T cells expressing ddVenus were plated in 1 mL of media at 400,000 cells per well in 12-well plates and allowed to adhere overnight. Cells were treated with DMSO or cycloheximide (20 μg/mL) for 15 min at 37 °C, followed by addition of MG-132 (4 μM) in the presence or absence of mycolactone (100 nM) or CB-5083 (1 μM). Note that when added, cycloheximide was present throughout the experiment. At the indicated time points, cells were harvested by pipetting with an aliquot saved for flow cytometry, washed twice in ice cold PBS, and frozen at −20 °C. Cells or cell lysates were analyzed by flow cytometry or Western blot as above.

Proteomic Analysis. MutuDCs (4.10^6 cells) were treated with 100 nM mycolactone or DMSO as a vehicle control for 6 or 24 h, in triplicate. Cells from each condition were harvested and washed twice with PBS, and cell pellets were frozen at −80 °C until further use. Cell pellets were resuspended in 500 μL of lysis buffer [9 M urea, 20 mM Hepes (pH 8.0), phosSTOP tablet (one tablet in 10 mL of buffer; Roche)], sonicated (three bursts of 15 s at an amplitude of 20%), and centrifuged for 15 min at 16,000 × *g* at 4 °C to remove insoluble material. The protein concentration in the supernatants was measured using a Bradford assay (Bio-Rad), and 0.5 mg of total protein in each sample was used to continue the protocol. Proteins in each sample were reduced by addition of 5 mM DTT and incubation for 30 min at 55 °C, and were then alkylated by addition of 100 mM iodoacetamide for 15 min at RT in the dark. Both samples were further diluted with 20 mM Hepes (pH 8.0) to a final urea concentration of 4 M, and proteins were digested with 2 μg of LysC (Wako) (1:250, wt/wt) for 4 h at 37 °C. Samples were again diluted to 2 M urea and digested with 5 μg of trypsin (Promega) (1:100, wt/wt) overnight at 37 °C. The resulting peptide mixture was acidified by

addition of 1% TFA, and after 15 min of incubation on ice, samples were centrifuged for 15 min at 1,780 × *g* at RT to remove insoluble components. Next, peptides were purified on SampliQ C18 cartridges (Agilent). Cartridges were first washed with 1 mL of 100% acetonitrile (ACN) and preequilibrated with 3 mL of solvent A [25 μL of 0.1% TFA in water/ACN (98:2, vol/vol)] before samples were loaded on the cartridge. After peptide binding, the column was washed again with 2 mL of solvent A and peptides were eluted with 700 μL of 0.1% TFA in water/ACN (20:80, vol/vol). Purified peptides were redissolved in solvent A, and 10 μL was injected for LC-MS/MS analysis on an Ultimate 3000 RSLCnano System (Dionex; Thermo Fisher Scientific) connected in-line to a Q Exactive HF mass spectrometer with a Nanospray Flex Ion source (Thermo Fisher Scientific). Trapping was performed at 10 $\mu L \cdot min^{-1}$ for 4 min in solvent A [on a reverse-phase column produced in-house (100-μm i.d. × 20 mm) using 5-μm beads (C18 Reprosil-Pur; Dr. Maisch)], followed by loading the sample on a 40-cm column packed in the needle [produced in-house (75 μm i.d. × 400 mm) using 1.9-μm beads (C18 Reprosil-HD; Dr. Maisch)]. Peptides were eluted by an increase in solvent B [0.1% formic acid in water/ACN (2:8, vol/vol)] in linear gradients from 2 to 30% in 100 min, then from 30 to 56% in 40 min, and finally from 56 to 99% in 5 min, all at a constant flow rate of 250 $nL \cdot min^{-1}$. The mass spectrometer was operated in the data-dependent mode, automatically switching between MS and MS/MS acquisition for the 16 most abundant ion peaks per MS spectrum. Full-scan MS spectra (375–1,500 *m/z*) were acquired at a resolution of 60,000 after accumulation to a target value of 3 million, with a maximum fill time of 60 ms. The 16 most intense ions above a threshold value of 22,000 were isolated [window of 1.5 thomson (Th)] for fragmentation at a normalized collision energy of 32% after filling the trap at a target value of 100,000 for a maximum of 45 ms. The S-lens RF level was set at 55, and we excluded precursor ions with single and unassigned charge states.

Data Processing and Analysis. Data analysis was performed with MaxQuant (version 1.5.3.30) (38) using the Andromeda search engine with default search settings, including a false discovery rate (FDR) set at 1% on both the peptide and protein levels. Spectra were searched against the mouse proteins in the UniProt database (database version of April 2016 containing 16,622 mouse protein sequences; www.uniprot.org) with a mass tolerance for precursor and fragment ions of 4.5 ppm and 20 ppm, respectively, during the main search. Enzyme specificity was set as C-terminal to arginine and lysine, also allowing cleavage at proline bonds and a maximum of two missed cleavages. Variable modifications were set to oxidation of methionine residues and acetylation of protein N termini. Carbamidomethyl formation of cysteine residues was set as a fixed modification. Proteins with at least one unique or razor peptide were retained and then quantified by the MaxLFQ algorithm integrated into the MaxQuant software (39). A minimum ratio count of two unique or razor peptides was required for quantification. Further data analysis was performed with Perseus software (version 1.5.4.1) after loading the protein groups file from MaxQuant. Proteins only identified by site, reverse database hits, and potential contaminants were removed, and replicate samples were grouped. Proteins with less than three valid values in at least one group were removed, and missing values were imputed from a normal distribution around the detection limit. The statistical analysis to determine differentially expressed proteins was performed with R software (version 3.3.2) using the *limma* package. *P* values were corrected for multiple testing using the Benjamini–Hochberg method to obtain an FDR. Proteins with an FDR ≤ 0.1 and a $\log_2$ mycolactone/control LFQ intensity fold change ($\log_2$ FC) > 0.5 were considered up-regulated by mycolactone, whereas proteins with an FDR ≥ 0.1 and a $\log_2$ FC < -0.5 were considered down-regulated. The MS proteomics data have been deposited to the ProteomeXchange Consortium via the PRIDE partner repository (40, 41) with the dataset identifier PXD006103. Gene ontology annotations of proteins were inferred from the UniProt database.

ACKNOWLEDGMENTS. C.D. received funding from the Institut Pasteur, INSERM, and Fondation Raoul Follereau. J.-D.M. is the recipient of a doctoral fellowship from the Ecole Normale Supérieure de Lyon. S.A. received funding from the Institute Curie, INSERM, CNRS, la Ligue Contre le Cancer (Equipe labellisée Ligue, EL2014.LNCC/SA), Association pour la Recherche contre le Cancer, European Research Council (2013-AdG 340046 DCBIOX), Institut National du Cancer PLBIO13-057, Agence Nationale de la Recherche (ANR)-11-LABX-0043, ANR-10-IDEX-0001-02 PSL, ANR-16-CE15001801, and ANR-16-CE18002003. P.K. was supported by European Molecular Biology Organization (ALTF 467-2012) and the Wellcome Trust (101578/Z/13/Z). F.I. was supported by Odysseus Grant G0F8616N from the Research Foundation of Flanders. Work by J.E.G. and P.C. was supported by NIH Grant R01-AI097206.

1. Mellman I (2013) Dendritic cells: Master regulators of the immune response. *Cancer Immunol Res* 1:145–149.
2. Joffre OP, Segura E, Savina A, Amigorena S (2012) Cross-presentation by dendritic cells. *Nat Rev Immunol* 12:557–569.
3. Alloatti A, Kotsias F, Magalhaes JG, Amigorena S (2016) Dendritic cell maturation and cross-presentation: Timing matters! *Immunol Rev* 272:97–108.
4. Grotzke JE, Cresswell P (2015) Are ERAD components involved in cross-presentation? *Mol Immunol* 68:112–115.
5. Vembar SS, Brodsky JL (2008) One step at a time: Endoplasmic reticulum-associated degradation. *Nat Rev Mol Cell Biol* 9:944–957.
6. Tretter T, et al. (2013) ERAD and protein import defects in a sec61 mutant lacking ER-lumenal loop 7. *BMC Cell Biol* 14:56.
7. Kaiser ML, Römisch K (2015) Proteasome 19S RP binding to the Sec61 channel plays a key role in ERAD. *PLoS One* 10:e0117260.
8. Stein A, Ruggiano A, Carvalho P, Rapoport TA (2014) Key steps in ERAD of luminal ER proteins reconstituted with purified components. *Cell* 158:1375–1388.
9. Ackerman AL, Giodini A, Cresswell P (2006) A role for the endoplasmic reticulum protein retrotranslocation machinery during crosspresentation by dendritic cells. *Immunity* 25:607–617.
10. Amigorena S, Savina A (2010) Intracellular mechanisms of antigen cross presentation in dendritic cells. *Curr Opin Immunol* 22:109–117.
11. Imai J, Hasegawa H, Maruya M, Koyasu S, Yahara I (2005) Exogenous antigens are processed through the endoplasmic reticulum-associated degradation (ERAD) in cross-presentation by dendritic cells. *Int Immunol* 17:45–53.
12. Zehner M, et al. (2015) The translocon protein Sec61 mediates antigen transport from endosomes in the cytosol for cross-presentation to CD8(+) T cells. *Immunity* 42:850–863.
13. Baron L, et al. (2016) Mycolactone subverts immunity by selectively blocking the Sec61 translocon. *J Exp Med* 213:2885–2896.
14. George KM, et al. (1999) Mycolactone: A polyketide toxin from *Mycobacterium ulcerans* required for virulence. *Science* 283:854–857.
15. McKenna M, Simmonds RE, High S (2016) Mechanistic insights into the inhibition of Sec61-dependent co- and post-translational translocation by mycolactone. *J Cell Sci* 129:1404–1415.
16. McKenna M, Simmonds RE, High S (2017) Mycolactone reveals the substrate-driven complexity of Sec61-dependent transmembrane protein biogenesis. *J Cell Sci* 130:1307–1320.
17. Hall BS, et al. (2014) The pathogenic mechanism of the *Mycobacterium ulcerans* virulence factor, mycolactone, depends on blockade of protein translocation into the ER. *PLoS Pathog* 10:e1004061.
18. Kalies KU, Römisch K (2015) Inhibitors of protein translocation across the ER membrane. *Traffic* 16:1027–1038.
19. Fuertes Marraco SA, et al. (2012) Novel murine dendritic cell lines: A powerful auxiliary tool for dendritic cell research. *Front Immunol* 3:331.
20. Coutanceau E, et al. (2007) Selective suppression of dendritic cell functions by *Mycobacterium ulcerans* toxin mycolactone. *J Exp Med* 204:1395–1403.
21. Zlokarnik G, et al. (1998) Quantitation of transcription and clonal selection of single living cells with beta-lactamase as reporter. *Science* 279:84–88.
22. Grotzke JE, Lu Q, Cresswell P (2013) Deglycosylation-dependent fluorescent proteins provide unique tools for the study of ER-associated degradation. *Proc Natl Acad Sci USA* 110:3393–3398.
23. Anderson DJ, et al. (2015) Targeting the AAA ATPase p97 as an approach to treat cancer through disruption of protein homeostasis. *Cancer Cell* 28:653–665.
24. Sifers RN, Brashears-Macatee S, Kidd VJ, Muensch H, Woo SL (1988) A frameshift mutation results in a truncated alpha 1-antitrypsin that is retained within the rough endoplasmic reticulum. *J Biol Chem* 263:7330–7335.
25. Ackerman AL, Kyritsis C, Tampé R, Cresswell P (2003) Early phagosomes in dendritic cells form a cellular compartment sufficient for cross presentation of exogenous antigens. *Proc Natl Acad Sci USA* 100:12889–12894.
26. Guermonprez P, et al. (2003) ER-phagosome fusion defines an MHC class I cross-presentation compartment in dendritic cells. *Nature* 425:397–402.
27. Houde M, et al. (2003) Phagosomes are competent organelles for antigen cross-presentation. *Nature* 425:402–406.
28. Wiertz EJ, et al. (1996) Sec61-mediated transfer of a membrane protein from the endoplasmic reticulum to the proteasome for destruction. *Nature* 384:432–438.
29. Park E, Rapoport TA (2012) Mechanisms of Sec61/SecY-mediated protein translocation across membranes. *Annu Rev Biophys* 41:21–40.
30. Voorhees RM, Hegde RS (2016) Structure of the Sec61 channel opened by a signal sequence. *Science* 351:88–91.
31. Voorhees RM, Fernández IS, Scheres SH, Hegde RS (2014) Structure of the mammalian ribosome-Sec61 complex to 3.4 Å resolution. *Cell* 157:1632–1643.
32. Dingjan I, et al. (2016) Lipid peroxidation causes endosomal antigen release for cross-presentation. *Sci Rep* 6:22064.
33. Ploegh HL (2007) A lipid-based model for the creation of an escape hatch from the endoplasmic reticulum. *Nature* 448:435–438.
34. Bougnères L, et al. (2009) A role for lipid bodies in the cross-presentation of phagocytosed antigens by MHC class I in dendritic cells. *Immunity* 31:232–244.
35. Spangenberg T, Kishi Y (2010) Highly sensitive, operationally simple, cost/time effective detection of the mycolactones from the human pathogen *Mycobacterium ulcerans*. *Chem Commun (Camb)* 46:1410–1412.

36. Karttunen J, Sanderson S, Shastri N (1992) Detection of rare antigen-presenting cells by the lacZ T-cell activation assay suggests an expression cloning strategy for T-cell antigens. *Proc Natl Acad Sci USA* 89:6020–6024.
37. Denzin LK, Cresswell P (1995) HLA-DM induces CLIP dissociation from MHC class II alpha beta dimers and facilitates peptide loading. *Cell* 82:155–165.
38. Cox J, Mann M (2008) MaxQuant enables high peptide identification rates, individualized p.p.b.-range mass accuracies and proteome-wide protein quantification. *Nat Biotechnol* 26:1367–1372.
39. Cox J, et al. (2014) Accurate proteome-wide label-free quantification by delayed normalization and maximal peptide ratio extraction, termed MaxLFQ. *Mol Cell Proteomics* 13:2513–2526.
40. Vizcaíno JA, et al. (2016) 2016 update of the PRIDE database and its related tools. *Nucleic Acids Res* 44:D447–D456.
41. Vizcaíno JA, et al. (2014) ProteomeXchange provides globally coordinated proteomics data submission and dissemination. *Nat Biotechnol* 32: 223–226.